

Toward the Control of a Multi-Jointed, Monoped Runner

Uluç Saranlı, William J. Schwind* and Daniel E. Koditschek†
Department of Electrical Engineering and Computer Science
The University of Michigan
Ann Arbor, MI 48109-2110, USA

Abstract

In this paper, we propose a new family of controllers for multi-jointed planar monoped runners, based on approximate but accurate models of the stance phase dynamics of a two degree of freedom “SLIP” leg. Unlike previous approaches, the new scheme gives control over all parameters of the system including the hopping height, forward speed and duty cycle. The control laws are “deadbeat” in nature, derived by computing the inverse of an approximate return map and corrected by integral compensation. We use the expressions obtained in this way to control the original SLIP leg as well as radically different, more realistic four degree of freedom legs. In each case, the performance of the deadbeat scheme in controlling forward running velocity is compared to a modified Raibert control strategy, whose experimental stability properties have been analyzed carefully in the low degree of freedom setting.

1 Introduction

Biomechanists have gained great leverage in understanding basic principles of locomotion in creatures as diverse as humans and cockroaches by considering the “simple” SLIP model shown in Figure 1 as a metaphor for running and hopping [1, 3, 4, 5]. While simple to the biomechanist, even this model presents difficulties to the engineer wishing to pursue formal analysis and control since it is a hybrid system with nonlinear stance dynamics which are not closed-form integrable. Even so, previous work by two of the authors [15, 16] provides approximate functional relationships for the SLIP dynamics, enabling a consideration of control via established techniques.

The question remains, however, whether such consideration is warranted. Is the SLIP model any more than a metaphor for running and hopping? Is it actually a control target aimed for by humans and animals in spite of their greater degrees of freedom? If so, will the careful consideration of such a simple model allow

the engineer to create robots with dexterity reminiscent of humans and insects, or is this a “zoomorphic fallacy” tantamount to building a flying machine with flapping wings?

In answer to the former two questions, growing biological evidence, including recent work in our lab with human running data, suggests that the SLIP dynamics are more than just a metaphor. They are the literal control target for the center of mass of the subjects we have studied to date [14].

The latter question was in one sense answered by the landmark work of Raibert and his students [12] who used robots readily characterized by the SLIP model. The power of such simple leg models was demonstrated by the extensibility of the single leg ideas to two and four legged runners as well as the variety of behaviors generated: running with a number of gaits, jumping over obstacles, and performing acrobatic maneuvers. However, the legs used in this work were constructed to be SLIP-like. The question remains: Is it possible to use the simple SLIP model to characterize more complicated and biologically plausible leg models having ankle, knee and hip joints?

The biological evidence seems to provide a proof by existence. Additionally, intuition regarding the Lagrangian dynamics suggests that a “heavily-laden” higher degree of freedom leg will behave “almost identically” to a 2 DOF SLIP leg [16].

Given this evidence, this paper reports on our preliminary efforts to investigate the extensibility of SLIP based controllers to more complicated leg models.

1.1 Scope of the Paper: Coupled Controller for a “Special” SLIP Runner

The first work in the control of SLIP runners was the successful implementation by Raibert and his students [12] of simple, roughly decoupled controllers to independently control the hopping height and forward velocity of their robots. This stunning success motivated a series of papers [10, 17, 11, 15] characterizing the stability of these decoupled controllers.

In this paper we present a new coupled approximate deadbeat controller for a SLIP runner having a “special” spring potential model which makes a simplified version of the stance dynamics closed-form integrable.

*Supported in part by National Science Foundation Grant IRI-9612357

†Supported in part by National Science Foundation Grant IRI-9510673

We then explore the applicability of the decoupled controller (that we will term Raibert-like) and the new coupled controller in more biologically plausible legs.

1.2 Contributions of the Paper: The Power of the SLIP Model

In this paper we use simulation to suggest the possibility that control laws designed for SLIP leg, can be extended more biologically plausible leg models. As far as we know, this represents the first attempt to apply any 2 DOF derived return map controller to more complex single legs. We contrast a “deadbeat” and a Raibert-like controller in so doing.

It is not surprising to find that the approximate deadbeat controller outperforms the decoupled controller in the 2 DOF leg for which they were both developed.¹ It is surprising to find that the decoupled controller continues to function well in the 4 DOF leg. However, it seems to us truly noteworthy that the aggressive 2 DOF coupled controller can be adopted in the same way to the 4 DOF leg as well, even to the point of outperforming the decoupled algorithm. This significantly bolsters our suspicion that the “collapse of dimension” observed in biological control hierarchies might be explained in terms of isometries of the kind we have explored in [16].

Good performance can be achieved in the decoupled scheme when the gain parameters are tuned, whereas in contrast, the deadbeat controller is tuned automatically in its defining formula. Moreover, it allows for explicit control over duty factor².

Introducing the ability to explicitly command duty factor in addition to forward speed and hopping height may be useful when considering higher level control problems in dynamic locomotion such as foot placement on irregular terrain. Hodgins [7] studied the use of three different techniques for foot placement on irregular terrain: controlling forward speed, flight duration and stance duration. While we have not explored the implications of this work on foot placement in irregular terrain, the coupled controller’s ability to explicitly control forward speed, hopping height and duty factor will prove advantageous in such contexts.

2 The “Special” SLIP Runner

2.1 Model and Assumptions

The SLIP model considered in this paper is shown in Figure 1. The leg is assumed massless and the body

¹The tradeoffs between deadbeat and less model dependent controllers are well understood. The relative benefits in performance promised by the former can evaporate in the presence of noise and model mismatch that might not significantly undermine the latter.

²In fact, the introduction of the duty factor (the ratio of time a leg is on the ground over a complete cycle of leg movements) as a control objective is also a novelty of this work. While commonly considered in the biomechanics literature for either its power in classifying gait [2] or in its effect on metabolic efficiency, it has been all but ignored in the robotics literature.

	Lift-Off point
q_{rl}	Leg Length at Lift-Off
$q_{\theta l}$	Leg Angle at Lift-Off
\dot{q}_{rl}	Radial Velocity at Lift-Off
$\dot{q}_{\theta l}$	Angular Velocity at Lift-Off
	Apex Point
\bar{d}_y	Apex Hopping Height
\bar{d}_x	Apex Forward Velocity
ϕ	$\frac{TimeFlight}{TimeStance}$
	Touch-Down Point
q_{rt}	Leg Length at Touch-Down
$q_{\theta t}$	Leg Angle at Touch-Down
\dot{q}_{rt}	Radial Velocity at Touch-Down
$\dot{q}_{\theta t}$	Angular Velocity at Touch-Down

Table 1: Notation for the SLIP Leg Model

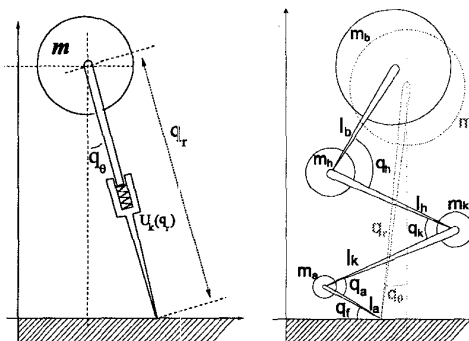


Figure 1: The spring loaded inverted pendulum (SLIP) leg model (left) and the “ankle-knee-hip” (AKH) leg model (right).

a point mass at the hip joint. During stance the leg is free to rotate around its toe and the mass is acted upon by a radial spring with potential $U(q_r)$. In flight, the mass is considered as a projectile acted upon by gravity. We assume there are no losses in either the stance or flight phases.

Despite its structural simplicity, the stance dynamics of this system are not integrable. Therefore, we begin our formal consideration by eliminating gravity from the stance dynamics yielding a simple central force problem wherein energy and angular momentum are both constants of motion and can be used to integrate the stance dynamics. The structure of the integrals suggest certain forms for the spring law which are physically realistic and also admit closed form integration [15, 16]. In particular, as in [15], we have chosen to work with the compressed air spring $U_A(q_r) = k/2(1/q_r^2 - 1/q_{r0}^2)$.

Before formulating the return map, we discuss the control inputs available for the SLIP runner. The first control input is the leg angle at touchdown, $q_{\theta t}$. We assume that during flight we are able to swing the leg to any desired angle relative to the ground. The other control inputs come from the ability to tune the spring

potential. In this work, we choose to tune the spring potential via choice of the stance compression and decompression spring constants, k_1 and k_2 , respectively.

2.2 The Control Objective

In formulating the control problem it is natural to work in the set of apex states (see Table 2 for state definitions),

$$\mathcal{X}_a = \{X_a \mid X_a = [\bar{b}_x, \bar{b}_y, \dot{\bar{b}}_x, \phi]^T\}$$

since its elements are easily observable and represent directly natural control specifications such as “jump this high” or “run this fast”.

Given this perspective, an obvious next step is to introduce the apex return map, $f_a : \mathcal{X}_a \times \mathcal{U}_k \mapsto \mathcal{X}_a$ where

$$\mathcal{U} = \{u \mid u = [q_{\theta t}, k_1, k_2]^T\}$$

is the set of control inputs. We are now in position to consider the coupled control problem.

That is, suppose we want to achieve the desired apex state (control objective),

$$X_a^* = [\bar{b}_x^*, \bar{b}_y^*, \dot{\bar{b}}_x^*, \phi^*]^T \quad (1)$$

One possible solution is the deadbeat control, that is, the control input $u^* = [q_{\theta t}^*, k_1^*, k_2^*]^T$ such that $X_a^* = f_a(X_a, u^*)$, effectively taking the current apex state X_a to the desired state X_a^* in one cycle.

The most direct way to find the deadbeat control u^* would be to invert the map f_a . However, the control inputs appear in the apex return map in a complicated manner making a direct computation of the inverse map difficult. In consequence, we introduce a new coordinate system, which affords an almost completely closed form inverse to an approximate return map.

2.3 The Liftoff Return Map

Consider the new state and control sets,

$$\mathcal{Z}_l = \{Z_l \mid Z_l = [q_{\theta l}, E_l, \psi_l, \phi]^T\}$$

$$\bar{\mathcal{U}} = \{\bar{u} \mid \bar{u} = [q_{\theta t}, a_1, \alpha]^T\}$$

where E_l is the energy at liftoff, ψ_l is the ratio of forward velocity to vertical velocity at liftoff and

$$a_i^2 := \frac{q_{rt}^2 \dot{q}_{\theta t}^2 + k_i / (m q_{rt}^2)}{\dot{q}_{rt}^2}; i = 1, 2 \quad (2)$$

$$\alpha^2 := \frac{a_2^2}{a_1^2} = \frac{q_{rt}^2 \dot{q}_{\theta t}^2 + k_1 / (m q_{rt}^2)}{q_{rt}^2 \dot{q}_{\theta t}^2 + k_2 / (m q_{rt}^2)} \quad (3)$$

Assuming $q_{rl} = q_{rt} = q_{r0}$, the liftoff return map

$f_l : \mathcal{Z}_l \times \bar{\mathcal{U}} \mapsto \mathcal{Z}_l$ can be written as³

$$f_l(Z_l, \bar{u}) := \begin{bmatrix} \vartheta_l \\ E_l + \Delta E_U + \Delta E_g \\ \mathbf{t}_{(1, -\vartheta_l)} \circ \mathbf{t}_{(\frac{1}{\alpha}, q_{\theta t})}(\psi_l) \\ \frac{t_f}{t_s} \end{bmatrix} \quad (4)$$

where

$$\vartheta_l = q_{\theta t} - \mathbf{t}_{(1, q_{\theta t})}(\psi_l) \left(\frac{\alpha + 1}{\alpha} \right) \frac{1}{a_1} \text{acot}(a_1) \quad (5)$$

$$\Delta E_U = U_{k_2}(q_r) - U_{k_1}(q_r) = \frac{1}{2} m \dot{q}_{rt}^2 (\alpha^2 - 1) \quad (6)$$

$$\Delta E_g = mg(q_{rl} \cos \vartheta_l - q_{rt} \cos q_{\theta t}) \quad (7)$$

$$t_f = \frac{1}{g} \sqrt{\frac{2}{m} \left(\frac{1}{\psi_l^2 + 1} \right) \left(\sqrt{E_l - mg q_{rl} \cos q_{\theta l}} - \sqrt{E_l + \psi_l^2 mg q_{rl} \cos q_{\theta l} - (1 + \psi_l^2) mg q_{rt} \cos q_{\theta t}} \right)} \quad (8)$$

$$t_s = \sqrt{\frac{q_{rt}^2}{\dot{q}_{rt}^2} \left(\frac{1}{1 + a_1^2} \right) \left(\frac{\alpha + 1}{\alpha} \right)} \quad (9)$$

and we define the following two parameter family of functions,

$$\mathbf{t}_{(\sigma_1, \sigma_2)}(\chi) := \tan(\sigma_1 \text{atan}(\chi) + \sigma_2). \quad (10)$$

Notice that apart from certain values of the parameters (e.g. $\sigma_1 = 1$ and $\sigma_2 = 0$) this family cannot be expressed in terms of a single elementary function. Finally note that both ψ_l and \dot{q}_{rt} , which appear in (4) can be expressed in terms of Z_l and $q_{\theta t}$.

3 The SLIP Deadbeat Controller

We want the ability to control the SLIP hopper to achieve a goal state,⁴

$$Z_l^* = [q_{\theta l}, E_l^*, \psi_l^*, \phi^*]^T \quad (11)$$

We are looking for the the deadbeat control, \bar{u}^* , such that

$$Z_l^* = f_l(Z_l, \bar{u}^*) \quad (12)$$

³Please refer to [13] for more details on the derivation of the liftoff map.

⁴As in Section 2.2 we can only choose three independent control objectives, here we select E_l , ψ_l and ϕ

3.1 Inverting the Return Map to Find Deadbeat Control

The simple form of the liftoff return map makes it possible, under a reasonable assumption, to reduce the inversion of f_l to the solution of a single equation in a single variable. The assumption that makes this possible is

$$\Delta E_g \equiv 0 \quad (13)$$

This assumption is reasonable in practice since ΔE_g appears in (4) only as a result of the unnatural energy discontinuities at touchdown and liftoff due to our no-gravity stance model, and does not appear in the stance dynamics with gravity.

Given this assumption, solution of the E_l and ϕ equations of (4) yields

$$\alpha^2(Z_l, Z_l^*, q_{\theta t}) = \frac{2}{m} \frac{E_l^* - E_l}{\dot{q}_{z_t}^2(Z_l, q_{\theta t})} + 1 \quad (14)$$

$$a_1^2(Z_l, Z_l^*, q_{\theta t}) = \quad (15)$$

$$\sqrt{\frac{q_{z_t}^2}{\dot{q}_{z_t}^2(Z_l, q_{\theta t})}} \left(\frac{\alpha(Z_l, Z_l^*, q_{\theta t}) + 1}{\alpha(Z_l, Z_l^*, q_{\theta t})} \right) \frac{\phi^*}{t_f(Z_l, q_{\theta t})} - 1$$

We then substitute both (14) and (15) into the ψ_l equation of (4) to arrive at a single equation in a single unknown variable, $q_{\theta t}$. Namely the equation

$$\psi_l^* = \mathbf{t}_{(1, -\partial_t(Z_l, Z_l^*, q_{\theta t}))^\circ} \mathbf{t}_{\left(\frac{-1}{\alpha(Z_l, Z_l^*, q_{\theta t})}, q_{\theta t}\right)}(\psi_l(Z_l, q_{\theta t})) \quad (16)$$

The function of $q_{\theta t}$ on the right hand side of the equation behaves nicely (e.g. it is monotone for most choices of Z_l, Z_l^*) and can be easily solved using numerical methods.

After solving for $q_{\theta t}$ from (16), we substitute the result into (14) and (15) to obtain α and a_1 . From here, it is trivial to go back to k_1 and k_2 , completing the inversion.

Finally, we can express the desired liftoff state, Z_l^* in terms of X_a^* and the control inputs [13]. Substituting the appropriate relationships, (16) becomes

$$\mathbf{t}_{(1, \partial_t(X_a, X_a^*, q_{\theta t}))}(\psi_l^*(X_a, X_a^*, q_{\theta t})) = \mathbf{t}_{\left(\frac{-1}{\alpha(X_a, X_a^*, q_{\theta t})}, q_{\theta t}\right)}(\psi_l(X_a, q_{\theta t})) \quad (17)$$

Equation (17) is used in the remainder of the paper to solve for $q_{\theta t}$ numerically (since no closed form expression involving elementary functions is available). This is in turn used to find k_1 and k_2 using the closed form expressions (2), (3), (15) and (14).

3.2 The Deadbeat and Modified Raibert Controllers

The procedure outlined in Section 3.1 gives an open loop approximate deadbeat controller for the ideal case where the plant exactly matches (save the omission of the ΔE_g term) the SLIP model with the compressed air spring introduced in Section 2.1.

Previous work by two of the authors [16] investigated the impact of the omission of gravity during

stance on the accuracy of the approximations and suggested possible corrections to the model. To minimize the effect of the prediction errors to controller performance, we augment the inverse apex map with a gravity correction policy, increasing the stance spring constants as a function of the gravitational potential at bottom [13]. The resulting control law is the approximate deadbeat controller we have been discussing.

For the purposes of comparison, we propose a decoupled alternative to this strategy based on Raibert's original control ideas. First, the forward velocity control is achieved by approximating a neutral leg placement and adjusting it with a proportional error term, yielding

$$q_{\theta t} = \text{asin}\left(\frac{\dot{x}t_s}{2q_{rt}} + k_{\dot{x}}(\bar{b}_x^* - \bar{b}_x)\right) \quad (18)$$

where $k_{\dot{x}}$ and the choice of \dot{x} are controller parameters. Next, we implement a Raibert-like hopping height controller by supplying the appropriate energy at bottom, via a change in spring constant $\Delta E_U = U_{k_2}(r_b) - U_{k_1}(r_b)$, in order to provide the energy difference between two successive apex points. In the absence of an estimate for r_b , we use measurements from previous strides. Similar to \dot{x} and $k_{\dot{x}}$, this is an estimation parameter which requires careful tuning for best performance.

Since both controllers, by their nature, will have tracking errors, we use integral feedback compensation, yielding a discrete closed loop system of the form

$$\begin{aligned} X_a[k+1] &= f_a(X_a[k], u_c(X_a[k], X_a^*[k+1] + e[k])) \\ e[k+1] &= e[k] + \frac{1}{c_i}(X_a^*[k] - X_a[k]) \end{aligned}$$

where $e[k]$ is the integral of the apex state error, $X_a^*[k]$ is the "reference" trace and $u_c(X_a, X_a^*)$ is a particular gait-level controller, in this paper, either the deadbeat or the modified Raibert controller.

3.3 Performance of the Deadbeat Controller

Even with integral compensation deadbeat control is an aggressive approach, imposing strong model dependence on the control law. In the absence of analytical results for the stability of the proposed controller in the presence of model mismatches, we explore in simulation the performance of the deadbeat controller and compare it to the benchmark of a modified Raibert control strategy. In particular, in Section 3.3.2, we begin by studying a simple SLIP, removing the assumption that gravity can be ignored during stance. We continue in Section 4.2 by considering two different four DOF legs having ankle, knee and hip joints and mass distributed throughout the leg.

Due to lack of space, this comparative study primarily focuses on the forward velocity behavior resulting from the control strategy. However, similar results are seen when considering the hopping height and duty factor behaviors [13].

3.3.1 Simulation Strategy

In this simulation study, we consider two families of waveforms we wish the apex velocity trace to track: one of step references and another of sinusoid references.

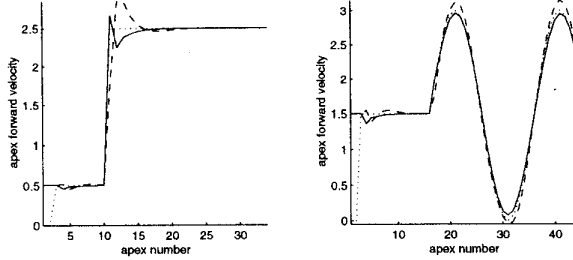


Figure 2: Sample runs of the deadbeat controller (solid lines) and modified Raibert (dashed lines) controllers applied to the 2 DOF SLIP leg for step and sinusoid references over 35 strides. Dotted lines represent the reference trace, while solid and dashed lines represent the actual performance of the SLIP runner.

Examples of both are shown in Figure 2. In each case, the hopper stabilizes around an initial running speed and the desired reference waveform is introduced at the end of 15 gait cycles.

When representing these references, we parameterize a step by its initial value and step amplitude and a sinusoid by its period and amplitude. Simulations are run over a range of these two dimensional parameter spaces. For a particular reference command, we summarize the control performance by the mean square error (MSE),

$$\text{MSE} = \frac{1}{N} \sum_{k=15}^N \|\ddot{b}_x^*[k] - \ddot{b}_x[k]\|^2$$

where N is the number of strides taken.

In presenting responses to these step and sinusoid reference command spaces, we collapse the initial velocity and sinusoid amplitude dimensions by averaging. In each case, 10 data points in the collapsed dimensions are chosen such that the forward velocity command always remains in the range $[0, 3]m/s$.

3.3.2 Simulation Results

Figure 3, summarizes the simulation data for step and sinusoid reference commands in forward velocity where we fix $\bar{b}_y^* = 1.2m$ and $\phi^* = 3$. The plots show the mean and variance of MSE for both controllers as a function of step amplitude (left) and sinusoid frequency (right). The results show that for this plant, the deadbeat controller provides better tracking than a modified Raibert controller. This observation about the control performance is not particular to the 2 DOF SLIP model, for we will see similar results for a 4 DOF AKH leg model in Section 4.2.

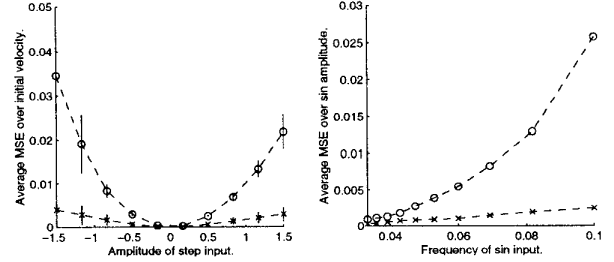


Figure 3: Step (left) and Sinusoid (right) References: The mean and variance of MSE as a function of the step amplitude (left) and sinusoid frequency (right), for the deadbeat (x) and modified Raibert (o) controllers. For this plant, $m = 50.48kg$, $\bar{b}_y^* = 1.2m$, $\phi^* = 3$.

Simulations with sinusoid reference commands reveal another property of the deadbeat controller. Due to its long settling time, the tracking error of the decoupled controller increases significantly for high frequency reference commands. The deadbeat controller, however, has shorter settling times — it ideally reaches the desired trajectory in one cycle — and consequently displays better tracking over a wide range of frequencies.

4 A More Realistic Leg Model

In this section, the application of the SLIP deadbeat controller to a much more complex dynamical leg structure, the four degree of freedom ankle/knee/hip model (Figure 1) is investigated. We consider two considerably different configurations of the four degree of freedom model: one with human-like and one with kangaroo-like kinematics and mass distribution. We present simulation evidence for the efficacy of the same approach as was used in Section 3.3.2 for the 2 DOF SLIP.

4.1 The 4 DOF AKH Leg Model

To simplify our thinking about this problem and make the application of the SLIP deadbeat controller as straightforward as possible, we consider a virtual SLIP leg connecting the toe of the 4 DOF leg to its center of mass (COM). The control objectives will remain the same as for the 2 DOF leg: the achievement of desired apex height, forward velocity and duty factor. The control implementation, however, will be considerably different, since the control inputs specified by the deadbeat controller, $u = [q_{\theta t}, k_1, k_2]^T$ are not directly transferable to the control inputs of the 4 DOF leg. Furthermore there is not a one to one correspondence between the 4 DOF leg angles and $q_{\theta t}$ nor between the joint torques and the virtual leg force.

Consequently, we must develop rules for choosing posture (the leg configuration) at touchdown to achieve the desired $q_{\theta t}$ and the joint torques during

stance to achieve the desired virtual leg stiffnesses, k_1 and k_2 . The manner in which we use biological evidence to guide the mathematical considerations used in forming these rules is presented in the next section.

4.2 Control of the AKH Leg

In controlling the four-jointed leg, we identify two levels, a joint level torque control, and an apex level virtual leg control.

Our controller attempts to force the COM trajectory of the 4 DOF leg to mimic a SLIP leg by proper choice of touchdown joint configuration and stance torques⁵. Our objective is to develop by closed loop joint controllers a “target leg” dynamics, yielding virtual leg dynamics as close as possible to SLIP dynamics. We accomplish this by constraining the work done by the joint torques to equal the work that would be done by a virtual spring between the toe and the center of mass, yielding

$$\bar{F}^T \dot{\bar{b}} = \tau^T \dot{q} \quad (19)$$

where \bar{F}^T and $\dot{\bar{b}}$ are the virtual spring force and the center of mass velocities respectively. Note that this is substantially different from forcing the center of mass to follow a prespecified target trajectory. The actual stance trajectory is still governed by AKH dynamics.

We then combine the torque constraint of (19) with a set of symmetry constraints of the form

$$\begin{bmatrix} 1 & -1 & 1 & -1 \\ 0 & \beta & -1 & 0 \end{bmatrix} q = \begin{bmatrix} -\gamma \\ 0 \end{bmatrix} \quad (20)$$

where β and γ are symmetry parameters, fixed for any particular locomotor. Intuitively, Equation 20 constrains the body link angle with respect to the ground to be γ , and the knee angle to be proportional to the ankle angle. In our simulations, the human-like leg has $\gamma = \pi/2$ and $\beta = 1$ and the kangaroo-like leg, has $\gamma = \pi/4$ and $\beta = 1$.

The leg configuration at touchdown is now completely specified, bridging the gap between the 4 dof leg model and the SLIP controller. As a consequence, we are able to use the controller principles explained in the preceding sections without any modifications. From the point of view of the apex controller, the combination of the torque control compensated leg dynamics are very close to SLIP dynamics.

We investigate the validity of this approach in simulation on two different 4 DOF legs, one human-like and one kangaroo-like whose structural parameters are given in Table 2.

As in Section 3.3.2 we issue step and sinusoid reference forward velocity commands and measure the tracking performance with the results shown in Figures 4 and 5, respectively. They support the validity of two major assumptions in the paper. First, they confirm that the SLIP model for running is applicable to significantly different kinematics and dynamics.

⁵Please refer to [13] for a detailed discussion.

	m_a, m_k, m_h, m_b	l_a, l_k, l_h, l_b
human	[26.4, 19.3, 3.5, 1.28]	[0.15, 0.35, 0.40, 0.35]
kangaroo	[30, 30, 5, 4]	[0.5, 0.7, 0.6, 0.5]

Table 2: Structural simulation parameters for human-like and kangaroo-like four degree of freedom legs [9].

Second, they suggest that, the connection between the SLIP model and the four-jointed complex model we consider does not rely on the particular “target pose”.

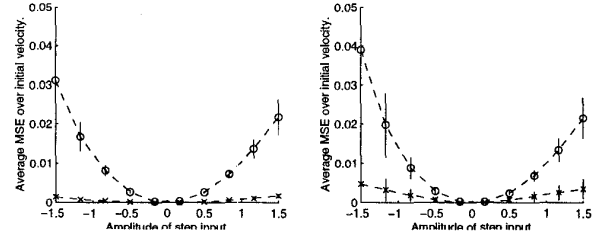


Figure 4: Step Reference: The mean and variance of MSE for human-like (left) and kangaroo-like (right) legs as a function of the step amplitude with the dead-beat(x) and modified Raibert(o) controllers. For this plant, $\bar{b}_y^* = 1.2m$, $\phi^* = 3$.

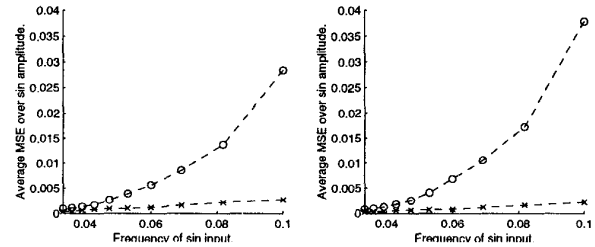


Figure 5: Sinusoid Reference: The mean of MSE for human-like (left) and kangaroo-like (right) legs as a function of the sinusoid frequency with the dead-beat(x) and modified Raibert(o) controllers. For this plant, $\bar{b}_y^* = 1.2m$, $\phi^* = 3$.

5 Conclusion

The present work serves as a tribute to the foresight of both those in the biomechanics community and those in the engineering community, such as Raibert, who have insisted that the SLIP model is the right place to begin thinking about dynamic locomotion. For not only is this model useful in describing the COM behavior of a multi-joint monopod runner as the biomechanists have claimed, but also for prescribing the control needed to achieve some desired behavior as Raibert

originally intuited. In particular, in this paper the control prescription arises from the extension of the 2 DOF SLIP deadbeat control to the higher degree of freedom AKH leg.

As far as we are aware, this is the first time that the SLIP model has been shown to be applicable to more zoomorphically realistic legs. Therefore, we believe this work will be of interest to both the engineering and biomechanics communities.

5.1 Relevance to Engineering

We witness in nature that advantage is conveyed to walkers and runners with higher degree of freedom legs. As such, while Raibert's robots demonstrated remarkable abilities, it seems certain in the long term that walking and running robots must be designed with higher degree of freedom legs. But not much work has been undertaken in building multi-degree of freedom runners, presumably because of the difficulty in "getting it right". Instead, research has progressed more rapidly in the direction of high degree of freedom dynamic animations, such as the exciting work by Hodgins and her students [8]. In either case, it would be useful to design easily tunable controllers in terms of high level behaviors, such as desired speed and hopping height.

We feel that the work presented in this paper is the first step in the direction of easily implementable, provably correct task based controllers for the high degree of freedom, zoomorphically realistic problem. We are encouraged by our current successes and hope to pursue the implementation of these deadbeat inspired controllers into dynamic simulations and experimental platforms with increasing degrees of freedom.

5.2 Relevance to Biomechanics

Given the almost universal ability to characterize an animal's COM behavior by the simple SLIP model, biomechanists are beginning to question how the many degrees of freedom are coordinated to mimic the 2 DOF SLIP [6]. In other words, they would like to identify the joint level controllers that in combination give the SLIP-like behavior of the COM. Given the difficulties of such a task and the absence of any other control strategies, we feel that the multi-joint deadbeat control strategy presented in this paper may serve as a good initial guide for addressing this problem.

Acknowledgements

We thank Prof. Claire Farley for a number of informative tutorial discussions on the biomechanics of human running. We also thank Prof. Jessica Hodgins and Dr. Nancy Pollard for their help with the 4 DOF simulations, in particular for providing the mass and kinematic data needed to make the human simulations more realistic.

References

- [1] R. M. Alexander. Three uses for springs in legged locomotion. *International Journal of Robotics Research*, 9(2):53-61, 1990.
- [2] R. M. Alexander and A. S. Jayes. Vertical movement in walking and running. *Journal of Zoology, London*, 185:27-40, 1978.
- [3] R. Blickhan. The spring-mass model for running and hopping. *Journal of Biomechanics*, 22:1217-1227, 1989.
- [4] R. Blickhan and R. J. Full. Similarity in multilegged locomotion: Bouncing like a monopode. *Journal of Comparative Physiology*, 173:509-517, 1993.
- [5] C. T. Farley, J. Glasheen, and T. A. McMahon. Running springs: Speed and animal size. *Journal of Experimental Biology*, 185:71-86, 1993.
- [6] C. T. Farley, H. P. Houdijk, C. van Strien, and M. Louie. Mechanisms for leg stiffness adjustment during bouncing gaits. 1997. In Review.
- [7] J. K. Hodgins. *Legged Robots on Rough Terrain: Experiments in Adjusting Step Length*. PhD thesis, Carnegie Mellon University, November 1989. CMU-CS-89-151.
- [8] J. K. Hodgins. Three-dimensional human running. In *ICRA*, Minneapolis, MN, May 1996.
- [9] J. K. Hodgins and N. S. Pollard. Typical human and kangaroo leg characteristics. Personal Communication.
- [10] D. E. Koditschek and M. Bühler. Analysis of a simplified hopping robot. *International Journal of Robotics Research*, 10(6):587-605, December 1991.
- [11] R. T. M'Closkey and J. W. Burdick. Periodic motions of a hopping robot with vertical and forward motion. *International Journal of Robotics Research*, 12(3):197-218, 1993.
- [12] M. H. Raibert. *Legged Robots That Balance*. MIT Press, Cambridge, MA, 1986.
- [13] U. Saranli and D. E. Koditschek. Analysis and control of slip and multi-jointed monoped planar hoppers. Technical report, EECS, UM, Ann Arbor, MI, 1998. In Preparation.
- [14] W. J. Schwind, C. T. Farley, and D. E. Koditschek. Identification of springs in human running, 1997. Paper in Progress.
- [15] W. J. Schwind and D. E. Koditschek. Control of forward velocity for a simplified planar hopping robot. In *Proceedings of the IEEE International Conference On Robotics and Automation*, Nagoya, Japan, May 1995.
- [16] W. J. Schwind and D. E. Koditschek. Characterization of monoped equilibrium gaits. In *Proceedings of the IEEE International Conference On Robotics and Automation*, Albuquerque, NM, April 1997.
- [17] A. F. Vakakis, J. W. Burdick, and T. K. Caughy. An 'interesting' strange attractor in the dynamics of a hopping robot. *International Journal of Robotics Research*, 10(6):606-618, December 1991.